Supplementary Information

Primitive Selection of the Fittest Emerging through Functional Synergy in Nucleopeptide Networks

Anil Kumar Bandela, Nathaniel Wagner, Hava Sadihov, Sara Morales-Reina, Agata Chotera-Ouda, Kingshuk Basu, Rivka Cohen-Luria, Andrés de la Escosura* and Gonen Ashkenasy*

* Department of Organic Chemistry, Universidad Autónoma de Madrid, Campus de Cantoblanco, 28049 Madrid, Spain. Email: andres.delaescosura@uam.es

* Department of Chemistry, Ben-Gurion University of the Negev, Beer-Sheva 84105, Israel. Email: gonenash@bgu.ac.il

Table of contents

Supplementary Methods

S1. General

Chemicals and reagents were purchased from Aldrich or Merck and were used without further purification unless otherwise specified. Amino acids, resins and coupling reagents were purchased from Novabiochem and Alfa Aesar, and DMF was purchased from Biotech Grade. Nucleic base precursors were purchased from Aldrich or Chem-Impex International.

S2. Synthesis and characterization

(a) Synthesis and characterization of P1 (see Scheme s1 in Supplementary Schemes and Figures section below).[1] Ethyl adenine-9-acetate (0.5 g, 2.21 mmol) and dimethyl amino pyridine (DMAP; 0.02 g, 0.164 mmol) were dissolved in dry THF (25 mL) in a N_2-flushed round bottom flask. Boc_2O (1.98 g, 9.10 mmol) was added to the stirred suspension, and the reaction mixture was stirred overnight at room temperature, and then halted when TLC analysis indicated complete consumption of the starting materials. The THF was removed by evaporation to give crude product as a yellow viscous material. The crude product was purified by column chromatography with CH_2Cl_2:CH_3OH (99:1) as eluent to get pure product as a pale-yellow sticky material (0.712 g; 76 %). ^{1}H NMR ($CDCl_3$): δ (ppm) = 8.86 (s, 1 H, Ar*H*), 8.14 (s, 1 H, Ar*H*), 5.04 (s, 2 H, ArC*H*$_2$CO), 4.27 (q, 2 H, CH_3C*H*$_2$O), 1.44 (s, 18 H, C(C*H*$_3$)$_3$) and 1.29 (t, 3 H, CH_2C*H*$_3$). ^{13}C NMR ($CDCl_3$): δ (ppm) = 166.6, 153.4, 152.3, 150.5, 150.3, 144.9, 128.3.4, 83.8, 62.5, 53.4, 44.3, 27.7 and 14.1. ESI-MS: m/z = 421 $[M]^+$. NMR and Mass spectra for **P1** are shown in Figure s1

(b) Synthesis and characterization of P2 (Scheme s1). 1N NaOH (1.83 mL, 1.04 mmol) was added slowly to a solution of **P1** (0.44 g, 1.04 mmol) in THF (10 mL) at 0 °C, and the reaction mixture was stirred for 30 min until TLC indicated complete consumption of the starting material, then quenched by the addition of H_2O (8.5 mL) and $KHSO_4$ (portion wise) to reach pH 3. The reaction mixture was poured into a separating funnel containing CH_2Cl_2 (40 mL). The organic phase was collected and dried with anhydrous Na_2SO_4, and the solvent was evaporated to dryness in vacuo. The pale-yellow oil turned to solid over night to give **2** (0.36 g, 87%) as an off-white solid. ^{1}H NMR ($CDCl_3$): δ (ppm) = 8.88 (s, 1 H, Ar*H*), 8.39 (s, 1 H, Ar*H*), 5.08 (s, 2 H, ArC*H*$_2$CO), 1.42 (s, 18 H, C(C*H*$_3$)$_3$). ^{13}C NMR ($CDCl_3$): δ (ppm) = 168.5, 153.3, 152.3, 150.3, 145.8, 127.5, 84.1, 44.3 and 27.8. ESI-MS: m/z = 393 $[M]^+$. NMR and Mass spectra for **P2** are shown in Figure s2.

(c) Synthesis and characterization of the electrophile E^{AA}

The electrophilic peptide **E^{AA}** was synthesized on solid phase MBHA.HCl resin using Boc-based chemistry with HBTU as the coupling agent. S-trityl protected mercaptopropionic acid was introduced onto the resin as the first amino acid followed by N,N boc protected diaminopropionic acid and finally by **P2** (2 eq.) as the last amino acid. After synthesis, the peptide was cleaved off the resin using TFMSA and proper scavengers and precipitated by cold ether and purified by preparative RP-HPLC, with a step gradient of solvents A (99 % water, 1 % acetonitrile and 0.1 % TFA) and B (90 % acetonitrile, 10 % water and 0.07 % TFA). The identity and purity of the peptides were then analyzed by analytical HPLC, ^{1}H NMR and LCMS. ^{1}H NMR (D_2O): δ (ppm) = 8.34 (d, J = 2 Hz, 2 H, Ar*H*), 8.25 (s, 1 H, Ar*H*), 8.23 (s, 1 H, Ar*H*), 5.18 (d, J = 3.2 Hz, 2 H, ArCH_2), 5.08 (d, J = 2.4 Hz, 2 H, ArCH_2), 4.73 (t, 1 H, NC*H*CH_2), 3.77 (dd, 1 H, NCH_2C*), 3.62 (dd, 1 H, NCH_2C*), 3.07 (t, 2 H, SCH_2CH_2), 2.49 (t, 2 H, COCH_2CH_2). ESI-MS: m/z = 542 $[M+H]^+$ and 564 $[M+Na]^+$. HPLC, NMR and Mass spectra for **E^{AA}** are shown in Figures s3 and s4.

(d) Synthesis and characterization of the electrophile E^{TT}

E^{TT} was synthesized in a way similar to **E^{AA}**, except that the last amino acid used for coupling was thymine-1-acetic acid (purchased from Aldrich).

^{1}H NMR (DMSO): δ (ppm) = 8.75 (d, 1 H, CON*H*CH), 8.24 (t, 1 H, CON*H*CH_2), 7.42 (s, 1 H, Ar*H*), 7.37 (s, 1 H, Ar*H*), 7.33 (s, 1 H, ArN*H*), 6.90 (s, 1 H, ArN*H*), 4.55 (q, 1 H, COC*H*), 4.36 (d, J = 8 Hz, 2 H, ArCH_2), 4.26 (d, J = 18.8 Hz, 2 H, ArCH_2) , 3.50 (m, 2 H, NCH_2C*), 2.94 (t, 2 H, SCH_2), 2.32 (t, 2 H, COCH_2), 1.74 (s, 6 H, ArCH_3). ESI-MS: m/z = 524 $[M+H]^+$. HPLC, NMR and Mass spectra for **E^{TT}** are shown in Figures s5 and s6.

(e) Synthesis and characterization of the electrophile E^{AT}

E^{AT} was synthesized in a slightly different way. Here, thymine 1-acetic acid was first coupled to N-boc protected diaminopropionic acid (Boc-Dap-OH), followed by coupling with the N-$(Boc)_2$ adenin-9-yl-acetic acid (**P2**). The N-adenine, N-thymine functionalized diaminopropionic acid was then coupled to mercaptopropionic acid immobilized on the solid phase MBHA.HCl. After synthesis, the peptide was cleaved off the resin using TFMSA and proper scavengers and precipitated by cold ether and purified by preparative RP-HPLC, with a step gradient of solvents A (99 % water, 1 % acetonitrile and 0.1 % TFA) and B (90 % acetonitrile, 10 % water and 0.07 % TFA). The identity and purity of the peptides were then analyzed by analytical HPLC, ^{1}H NMR and LCMS.

^{1}H NMR (D_2O): δ (ppm) = 8.26 (s, 1 H, Ar*H*), 8.15 (s, 1 H, Ar*H*), 7.27 (s, 1 H, Ar*H*), 4.99 (s, 2 H, ArCH_2CO), 4.43 (s, 2 H, ArCH_2CO), 3.67 (dd, 1 H, prochiral CH_2), 3.5 (dd, 1 H, prochiral CH_2), 2.99 (t, 2 H, SCH_2), 2.41 (t, 2 H, CCH_2CO), 1.72 (s, 3 H, ArCH_3). ESI-MS: m/z = 533 $[M+H]^+$. HPLC, NMR and Mass spectra for $\mathbf{E^{AT}}$ are shown in Figures s7 and s8.

(f) Synthesis of the replicator and nucleophile peptides

Replicator peptides ($\mathbf{R^{AA}}$, $\mathbf{R^{TT}}$, $\mathbf{R^{AT}}$) and the nucleophile (**N**) were synthesized on solid phase Rink-Amide resin using Fmoc-based chemistry with HBTU as the coupling agent. For synthesis of the replicators, orthogonally protected DPR (Fmoc-Dap(Dde)-OH) linker was used prior to coupling of the respective nucleobase carboxylic acids, N-$(Boc)_2$ adenin-9-yl-acetic acid for $\mathbf{R^{AA}}$, and thymine acetic acid for $\mathbf{R^{TT}}$. For $\mathbf{R^{AT}}$, N-$(Boc)_2$ adenin-9-yl-acetic acid and thymine acetic acid were coupled sequentially in an orthogonal fashion. Peptides were cleaved off the resin using trifluoroacetic acid (TFA) mixture with the proper scavengers, and then purified by preparative RP-HPLC, with a step gradient of solvents A (99 % water, 1 % acetonitrile and 0.1 % TFA) and B (90 % acetonitrile, 10 % water and 0.07 % TFA). The identity and purity of the peptides were then analyzed by analytical HPLC, and LCMS. HPLC and Mass spectra characterization of $\mathbf{R^{AA}}$, $\mathbf{R^{TT}}$ and $\mathbf{R^{AT}}$ are shown in Figures s9-s14 and characterization of **N** in Figures s15 and s16.

S3. Time dependent analysis of the replicator-assisted NCL reactions

Experiments were initiated by preparing mixtures containing **N** and the designated electrophile $\mathbf{E^{AA}}$ or $\mathbf{E^{TT}}$ (100 μM), the applied replicator $\mathbf{R^{AA}}$ or $\mathbf{R^{TT}}$ (30 or 60 μM), ABA as internal standard (30 μM) and TCEP (5 mM) as a reducing agent, in HEPES buffer pH 7.4. Total volume of the reaction mixture was 100 μL. Reactions were quenched at specific times in 30% acetic acid in water. The quenched reaction aliquots were analyzed by RP-HPLC.

S4. Time dependent analysis of the replicator-assisted NCL reactions in binary chemical networks (batch mode)

Experiments were initiated by preparing mixtures containing **N** (100 μM) and both $\mathbf{E^{AA}}$, $\mathbf{E^{TT}}$ (50 μM each), the applied replicator $\mathbf{R^{AA}}$ or $\mathbf{R^{TT}}$ (20 or 60 μM), ABA as internal standard (30 μM) and TCEP (5 mM) as a reducing agent, in HEPES buffer pH 7.4. Total volume of the reaction mixture was 100 μL. Reactions were quenched at specific times in 30% acetic acid in water. The quenched reaction aliquots were analyzed by RP-HPLC.

S5. Assembly structural characterization using AFM, TEM and fluorescence microscopy

(*i*) *Atomic force microscopy (AFM) imaging assays*: 3 µL aliquots from 60 µM solutions of $\mathbf{R^{AA}}$, $\mathbf{R^{TT}}$ or the mixture $\mathbf{R^{AA}}$:$\mathbf{R^{TT}}$ were deposited on a freshly cleaved mica surface (purchased from TED PELLA, INC.), and the samples were slowly dried in air overnight. Topography images were acquired by AFM (SolverPro, NT-MDT, Ru) in tapping mode using noncontact tips BudgetSensors Multi75Al-G, 3 Nm^{-1}, 75 kHz. Image processing, which included second order polynomial line fitting and cross-section analysis, was done using the NOVA AFM software. As a control, an AFM study was also performed for the NCL reactants ($\mathbf{E^{AA}}$, $\mathbf{E^{TT}}$ or **N**; 100 µM).. All images indicated the formation of spherical particles with diameters ranging 5-6 nm ($\mathbf{E^{AA}}$), ~4 nm ($\mathbf{E^{TT}}$) and ≤ 12 nm (**N**), as shown in Figure s21.

(*ii*) *Transmission electron microscopy (TEM) imaging assays*: TEM copper grids with 200-mesh carbon support (Electron Microscopy Sciences) were covered with 10 µL of the conjugate solution (60 µM) in 50 mM ammonium bicarbonate buffer pH 7.4, for 1 min. Then, the excess solution was wiped out with a filter paper. 10 µL of the staining solution, 2% uranyl acetate (Sigma–Aldrich) was added and incubated with the sample for 2 min; excess solution was again wiped away, and the grids were placed in desiccator to dry under vacuum. A Hitachi H-7500 transmission electron microscope was used to image the samples at 75 kV.

(*iii*) *Fluorescence microscopy imaging assays*: Samples were prepared by depositing 3 µL aliquots from 60 µM solutions of $\mathbf{R^{AA}}$, $\mathbf{R^{TT}}$ or mixture of $\mathbf{R^{AA}}$:$\mathbf{R^{TT}}$ that were incubated with Thioflavin T (ThT, 100 µM) for 15 min, on a glass slide and covered with coverslip. All the samples were scanned with 458 nm laser on Zeiss LSM 880 with Airyscan and processed in Fiji ImageJ program. In order to carry out the fluorescence recovery after photobleaching (FRAP) experiments, two droplets were chosen at a time, one for photo-bleaching and the other as reference. Bleaching and recovery experiment was done by instantly initiating a scan with maximal (100%) laser power, and then continue scanning with the optimal laser power for 30 s. The reference droplet was simply scanned with the optimal laser power for 30 s. FRAP results are shown in Fig. 3c in the manuscript and in Fig. s22c.

S6. Time dependent analysis of Thioflavin T binding to the self-assembled structures

Samples prepared with 60 µM total conjugate concentration, in 50 mM ammonium bicarbonate buffer pH 7.4. These samples were allowed 30 min for self-assembly, then incubated for additional 15 min in presence of 100 µM ThT; fluorescence spectra were then measured at different time intervals. The spectra were recorded on a 3001 Thermo Varioskan fluorescence

spectrometer, equipped with a 96-microwellplate reader. Spectra were collected from 465 to 700 nm, using an excitation wavelength of 440 nm (excitation slit width: 10 nm) at scan speed of 100 nm/min. The baseline of 100 μM ThT in the buffer was subtracted from the sample spectra. The typical fluorescence emission signals of ThT-bound fibers (481 nm) was used to compare the binding efficiency of the different assemblies.

S7. Modelling the mechanisms and kinetics of the network replication reactions

We support our network experiments with kinetic simulations that model the system according to the elementary steps of the individual reactions. In order to accurately follow the network behaviour, we used rate constants and system parameters that closely correspond to the experimental conditions, and initial concentrations used in the actual experiments. We ran the simulations for a variety of cases. First, we looked at the individual reactions (Fig. S24); this allowed us to confirm the validity of our kinetic model. Second, we looked at some of the network reactions and compared their results to our experimental results (Fig. 3c,d and Fig. s25); this further confirmed the validity of the model and its relevance to our network experiments. Third, we ran additional cases where experiments have not yet been conducted; this allows us to plan future experiments, and at times predict results for cases where experiments may be difficult to perform.

We have successfully used this procedure several times in the past.[2-5] Specifically, we have previously modelled β-sheet peptide networks that form fibril structures.[3,5] In this paper, our model also includes droplet structures, and, for the first time, the nucleopeptide networks.

Our simulations were performed by computing, in *MATLAB*, the kinetics of chemical reactions accounting for the reaction mechanism summarized in Figure 3b of the main manuscript, as outlined in the elementary reactions listed below. The following procedure was used: at incremental time steps, the extent of each reaction was calculated, and the concentrations of all reactants and products were then adjusted. This procedure was repeated at each time step. Mathematically, this is equivalent to solving the differential equations of the mass-action kinetics using the Euler method.[2,4]

$$F_i^A + F_1^A \underset{a_{-1}}{\overset{a^{AA}}{\rightleftharpoons}} F_{i+1}^A \qquad (i = 1, \ldots, n_A - 1)$$

$$B_j^T + B_1^T \underset{a_{-1}}{\overset{a^{TT}}{\rightleftharpoons}} B_{j+1}^T \qquad (j = 1, \ldots, n_T - 1)$$

$$F_i^{\mathbf{A}} \xrightarrow{d^{AA}} F_{i/2}^{\mathbf{A}} + F_{i/2}^{\mathbf{A}} \qquad (i = 10m_A, \ldots, n_A)$$

$$B_j^{\mathbf{T}} \xrightarrow{d^{TT}} B_{j/2}^{\mathbf{T}} + B_{j/2}^{\mathbf{T}} \qquad (j = 10m_T, \ldots, n_T)$$

$$E^{\mathbf{A}} + N \xrightarrow{g^A} F_1^{\mathbf{A}}$$

$$E^{\mathbf{T}} + N \xrightarrow{g^T} B_1^{\mathbf{T}}$$

$$E^{\mathbf{A}} + N + F_i^{\mathbf{A}} \xrightarrow{b^{AA}} F_{i+1}^{\mathbf{A}} \qquad (i = m_A, \ldots, n_A - 1)$$

$$E^{\mathbf{T}} + N + B_j^{\mathbf{T}} \xrightarrow{b^{TT}} B_{j+1}^{\mathbf{T}} \qquad (j = m_T, \ldots, n_T - 1)$$

$$E^{\mathbf{A}} + N + B_j^{\mathbf{T}} \xrightarrow{b^{AT}} F_1^{\mathbf{A}} + B_j^{\mathbf{T}} \qquad (j = m_T, \ldots, n_T)$$

$$E^{\mathbf{T}} + N + F_i^{\mathbf{A}} \xrightarrow{b^{TA}} B_1^{\mathbf{T}} + F_i^{\mathbf{A}} \qquad (i = m_A, \ldots, n_A)$$

$$F_i^{\mathbf{A}} : \; i = 1, \ldots, n_A \qquad B_j^{\mathbf{T}} : \; j = 1, \ldots, n_T$$

$$T_{TOT}^{\mathbf{A}} = \sum_{i=1}^{n_A} i\left[F_i^{\mathbf{A}}\right] \qquad T_{TOT}^{\mathbf{T}} = \sum_{j=1}^{n_T} j\left[B_j^{\mathbf{T}}\right]$$

Here, F_i^A refers to $\mathbf{R^{AA}}$ fibrils of length i monomers, while B_j^T refers to $\mathbf{R^{TT}}$ spherical objects containing j monomers. m_A and m_T are parameters that describe the minimal aggregate seeds of the fibrils and droplets, respectively.[3] $\mathbf{R^{AA}}$ and $\mathbf{R^{TT}}$ monomers are also produced by the background reactions. Large fibrils and droplets may decompose into two smaller equal segments, from sizes 10 m_A and 10 m_T and above, respectively. n_A and n_T are the respective maximum sizes of the fibrils and droplets. The last line describes the computation of the total concentrations of $\mathbf{R^{AA}}$ and $\mathbf{R^{TT}}$ monomers in all forms

Table s1 below lists all the cases we ran. Unless explicitly listed in the table, the following default parameters and rate constants were used:

$g^A = g^T = 1 \quad a^{AA} = 10000 \quad a^{TT} = 1000 \quad a_{-1} = 0.01$

$b^{AA} = 1000000 \qquad (\mathrm{i} = \mathrm{m}_A, \ldots, \mathrm{n}_A - 1)$

$b^{TT} = 1000 \qquad (\mathrm{j} = \mathrm{m}_T, \ldots, \mathrm{n}_T - 1)$

$b^{AT} = 10000000 \qquad (\mathrm{j} = \mathrm{m}_T, \ldots, \mathrm{n}_T)$

$b^{TA} = 100000 \qquad (\mathrm{i} = \mathrm{m}_A, \ldots, \mathrm{n}_A)$

$d^{AA} = 1 \qquad (\mathrm{i} = 10\mathrm{m}_A, \ldots, \mathrm{n}_A)$

$d^{TT} = 1 \qquad (\mathrm{j} = 10\mathrm{m}_T, \ldots, \mathrm{n}_T)$

$\mathrm{F}_{\mathrm{i}}^{\mathbf{A}} : \mathrm{i} = 1, \ldots, \mathrm{n}_A \qquad \mathrm{B}_{\mathrm{j}}^{\mathbf{T}} : \mathrm{j} = 1, \ldots, \mathrm{n}_T$

$\mathrm{m}_A = \mathrm{m}_T = 10 \qquad \mathrm{n}_A = \mathrm{n}_T = 1000$

The units of the *g* and *a* type rate constants are M^{-1} hr^{-1}.
The units of the *b* rate constants are M^{-2} hr^{-1}.
The units of a_{-1} and the *d* type rate constants are hr^{-1}.

The Matlab function *simbetaa* used to run the simulation is listed below. As in the Euler method, the steps in the code correspond to time increments in the mass-action kinetics.

```
function sout = simbetaa (m_a, m_t, n_a, n_t, srate, sinit, maxtime, dtime)
% function sout = simbetaa (m_a, m_t, n_a, n_t, srate, sinit, maxtime, dtime)
% simbetaa: simulation function
% concentrations: Ea, Et, N, Fa[1<->n_a], Bt[1<->n_t], Ta[1<->n_d], Tt[1<->n_d]
% rate constants: aaa, att, a_r, daa, dtt, ga, gt, baa, btt, bat, bta
% maxtime: maximum time, dtime: delta time
%
one2na=1:n_a; one2na1=1:(n_a-1); two2na=2:n_a;
ma2na=m_a:n_a; ma2na1=m_a:(n_a-1); ma12na=(m_a+1):n_a;
tenma2na=(10*m_a):n_a; tenma2naf=floor(tenma2na/2); tenma2nac=ceil(tenma2na/2);
one2nt=1:n_t; one2nt1=1:(n_t-1); two2nt=2:n_t; mt2nt=m_t:n_t;
mt2nt1=m_t:(n_t-1); mt12nt=(m_t+1):n_t;
tenmt2nt=(10*m_t):n_t; tenmt2ntf=floor(tenmt2nt/2); tenmt2ntc=ceil(tenmt2nt/2);
time=dtime:dtime:maxtime; ltime=length(time);
aaa=srate.aaa; att=srate.att; a_r=srate.a_r;
daa=srate.daa; dtt=srate.dtt;
ga=srate.ga; gt=srate.gt;
baa=srate.baa; btt=srate.btt; bat=srate.bat; bta=srate.bta;
Ea=sinit.Ea; Et=sinit.Et; N=sinit.N;
Fa=[sinit.Fa;zeros(n_a-1,1)]; Bt=[sinit.Bt;zeros(n_t-1,1)];
sout.Ta=zeros(1,ltime); sout.Tt=zeros(1,ltime);
%
for itime=1:ltime
   naaa=dtime*(aaa*Fa(1)*Fa(one2na1)-a_r*Fa(two2na));
   natt=dtime*(att*Bt(1)*Bt(one2nt1)-a_r*Bt(two2nt));
   ndaa=dtime*daa*Fa(tenma2na);
   ndtt=dtime*dtt*Bt(tenmt2nt);
   nga=dtime*ga*Ea*N;
   ngt=dtime*gt*Et*N;
   nbaa=dtime*baa*Ea*N*Fa(ma2na1);
   nbtt=dtime*btt*Et*N*Bt(mt2nt1);
   nbat=dtime*bat*Ea*N*Bt(mt2nt);
   nbta=dtime*bta*Et*N*Fa(ma2na);
   %
   dEa=nga+sum(nbaa)+sum(nbat);
   dEt=ngt+sum(nbtt)+sum(nbta);
   Ea=Ea-dEa; Et=Et-dEt; N=N-dEa-dEt;
   Fa(1)=Fa(1)-sum(naaa)+nga+sum(nbat);
   Bt(1)=Bt(1)-sum(natt)+ngt+sum(nbta);
   %
   Fa(one2na1)=Fa(one2na1)-naaa;
   Bt(one2nt1)=Bt(one2nt1)-natt;
   Fa(two2na)=Fa(two2na)+naaa;
   Bt(two2nt)=Bt(two2nt)+natt;
   %
   Fa(tenma2na)=Fa(tenma2na)-ndaa;
   Bt(tenmt2nt)=Bt(tenmt2nt)-ndtt;
   Fa(tenma2naf)=Fa(tenma2naf)+ndaa;
   Fa(tenma2nac)=Fa(tenma2nac)+ndaa;
   Bt(tenmt2ntf)=Bt(tenmt2ntf)+ndtt;
   Bt(tenmt2ntc)=Bt(tenmt2ntc)+ndtt;
   %
   Fa(ma2na1)=Fa(ma2na1)-nbaa;
   Fa(ma12na)=Fa(ma12na)+nbaa;
   Bt(mt2nt1)=Bt(mt2nt1)-nbtt;
   Bt(mt12nt)=Bt(mt12nt)+nbtt;
   %
   sout.Ta(itime)=one2na*Fa; sout.Tt(itime)=one2nt*Bt;
   sout.Ea=Ea; sout.Et=Et; sout.N=N;
   sout.Fa=Fa; sout.Bt=Bt;
   %
   if any([Ea;Et;N;Fa;Bt]<0)
      disp('Renormalize'); disp(['time = ',num2str(itime*dtime)]); break;
   end
end
```

S8. Time dependent analysis of the replicator-assisted reaction networks far from equilibrium

(i) *Network reaction assays in the flow reactor (**E^{AA}:E^{TT}:N = 1:1:2**)*: The flow cell device contained three inlets fitted with three syringes (Fig. 4a of the manuscript) of which one contained **N** ± **R** (**N** = 100 μM; **R** = 20 μM in HEPES buffer pH 7.4 containing TCEP as reducing agent), the other with $\mathbf{E^{AA}}$ (50 μM) and the third with $\mathbf{E^{TT}}$ (50 μM) and **ABA** (30 μM). The volume of the all three syringes was 210 μL each and each solution was injected with a constant flow rate of 14.8 (μL/h). Reactions were quenched by collecting the drops coming from the chamber outlet into 30% acetic acid in water. Quenched reaction aliquots were analyzed by RP-HPLC. For analysis, the concentration of the product at t = 0 (right before flow starts) was taken as zero.

(ii) *Network reaction assays in the flow reactor (**E^{AA}:E^{TT}:N = 1:1:1**)*: the experimental set-up was the same as in (*i*) except for that **N**, $\mathbf{E^{AA}}$ and $\mathbf{E^{TT}}$ were 67 μM each.

(iii) *Network reaction assays in the flow reactor (**E^{AA}:E^{TT}:N = 1:1:1**) in presence of inhibitors*: the experimental set-up was same as in (*ii*) with an extra component, the applied inhibitor, injected from the central inlet.

Table s1. The parameters {initial concentrations, rate constants (g) and seeding (m)} used for each run.

Simulation	N (μM)	E^{AA} (μM)	E^{TT} (μM)	R^{TT} (μM)	R^{AA} (μM)	g	m_A	m_T	Figure
Individual reactions	100	100	0	0	0	1	10	10	s24
	100	100	0	30	0	1	10	10	
	100	100	0	60	0	1	10	10	
	100	100	0	0	30	1	10	10	
	100	100	0	0	60	1	10	10	
	100	0	100	0	0	1	10	10	
	100	0	100	30	0	1	10	10	
	100	0	100	60	0	1	10	10	
	100	0	100	0	30	1	10	10	
	100	0	100	0	60	1	10	10	
Reaction Networks									
Native	100	50	50	0	0	1	10	10	s25
	100	50	50	20	0	1	10	10	3c
	100	50	50	60	0	1	10	10	
	100	50	50	0	20	1	10	10	3d
	100	50	50	0	60	1	10	10	
	100	50	50	10	10	1	10	10	s25
	100	50	50	30	30	1	10	10	
Competitive	67	67	67	0	0	1	10	10	s26
	67	67	67	20	0	1	10	10	3e
	67	67	67	60	0	1	10	10	
	67	67	67	0	20	1	10	10	3f
	67	67	67	0	60	1	10	10	
	67	67	67	10	10	1	10	10	s26
	67	67	67	30	30	1	10	10	
Inactive bg	100	50	50	0	0	0.1	10	10	s27
	100	50	50	20	0	0.1	10	10	3g
	100	50	50	60	0	0.1	10	10	
	100	50	50	0	20	0.1	10	10	3h
	100	50	50	0	60	0.1	10	10	
Active seeding	100	50	50	0	0	1	25	5	s28
	100	50	50	20	0	1	25	5	3i
	100	50	50	60	0	1	25	5	
	100	50	50	0	20	1	25	5	s28
	100	50	50	0	60	1	25	5	
	100	50	50	0	0	1	5	25	s29
	100	50	50	20	0	1	5	25	
	100	50	50	60	0	1	5	25	
	100	50	50	0	20	1	5	25	3j
	100	50	50	0	60	1	5	25	

Supplementary Schemes and Figures

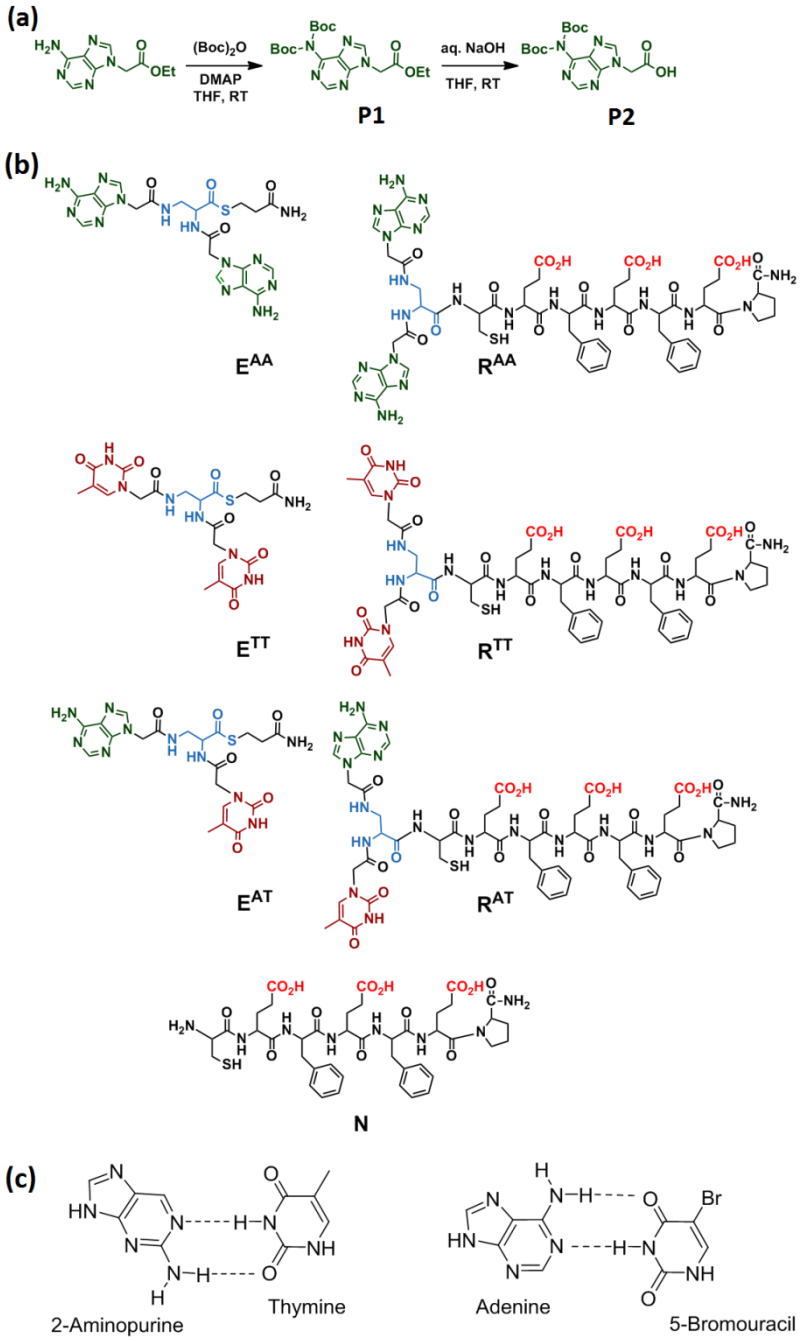

Scheme s1: (a) Synthesis of the N-(Boc)$_2$ adenin-9-yl-acetic acid (**P2**). (b) Chemical structures of the synthesized electrophilic (**E^{AA}**, **E^{TT}**, **E^{AT}**), nucleophilic (**N**) and replicator nucleopeptide molecules (**R^{AA}**, **R^{TT}** and **R^{AT}**). At pH 7.4 the Glu side chain carboxylic acids would be in their deprotonated anionic form. (c) Watson-crick base pairing mode of 2-aminopurine with thymine, and 5-bromouracil with adenine.

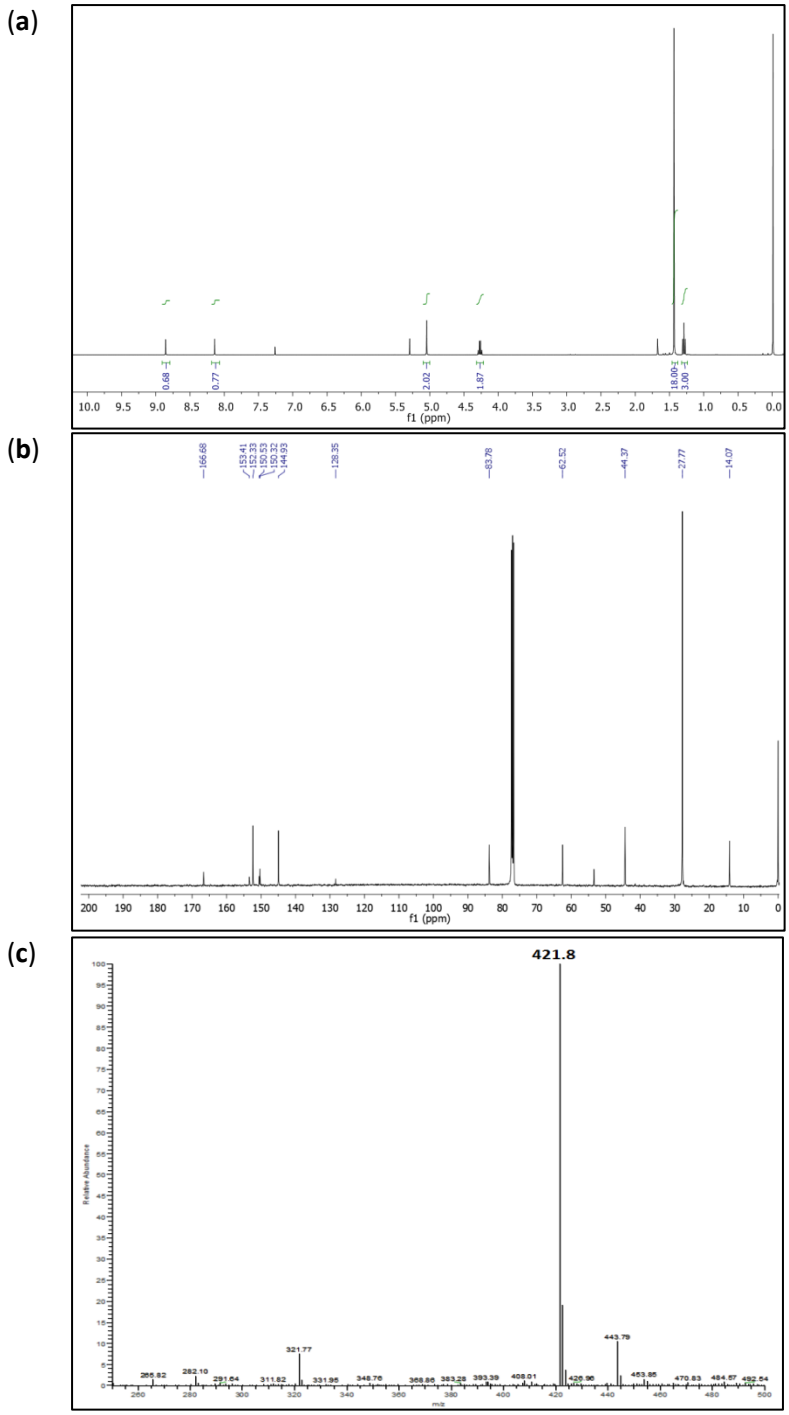

Figure s1. (a) ^{1}H NMR spectrum of **P1** in $CDCl_3$. (b) ^{13}C NMR spectrum of **P1** in $CDCl_3$. (c) Electron spray mass spectrometry (ESI-MS) of **P1**. Calculated m/z = 421 $[M]^+$.

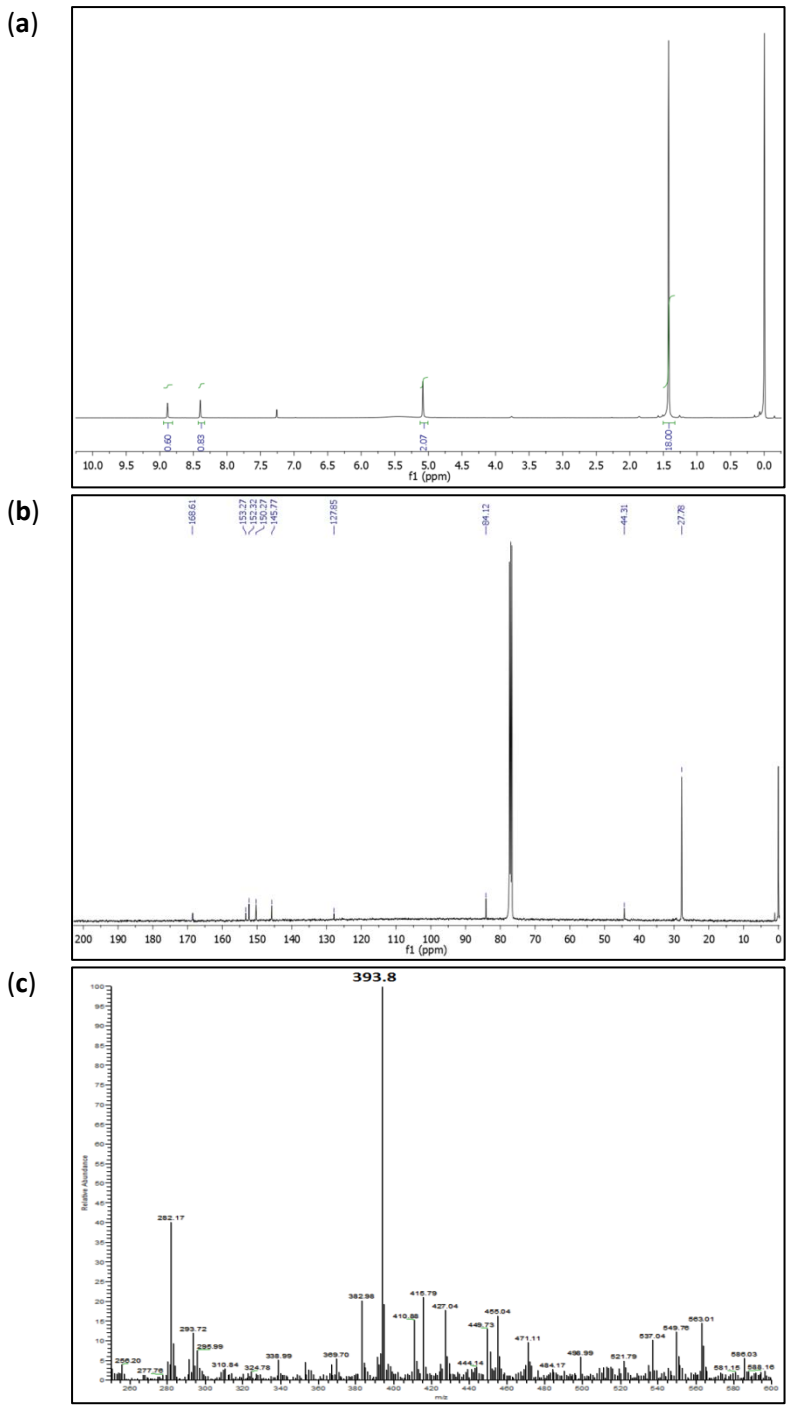

Figure s2. (a) ^{1}H NMR spectrum of **P2** in $CDCl_3$. (b) ^{13}C NMR spectrum of **P2** in $CDCl_3$. (c) ESI-MS of **P2**. Calculated m/z = 393 $[M]^+$.

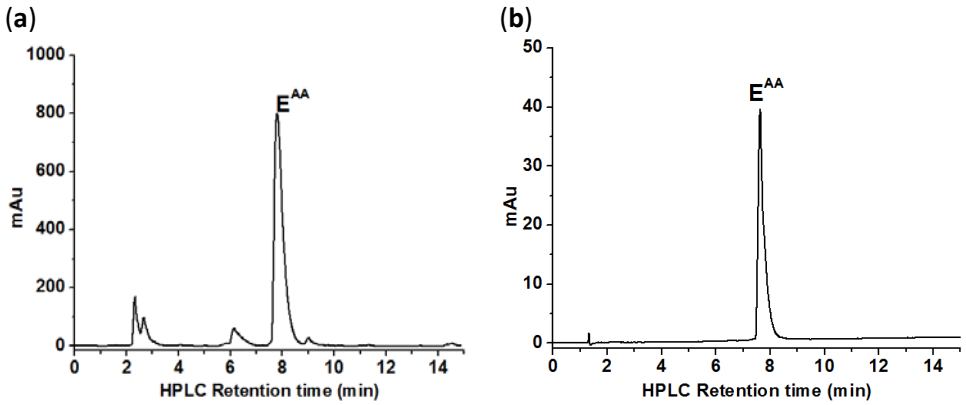

Figure s3. HPLC chromatograms of $\mathbf{E^{AA}}$. (a) Crude obtained after synthesis; (b) After purification.

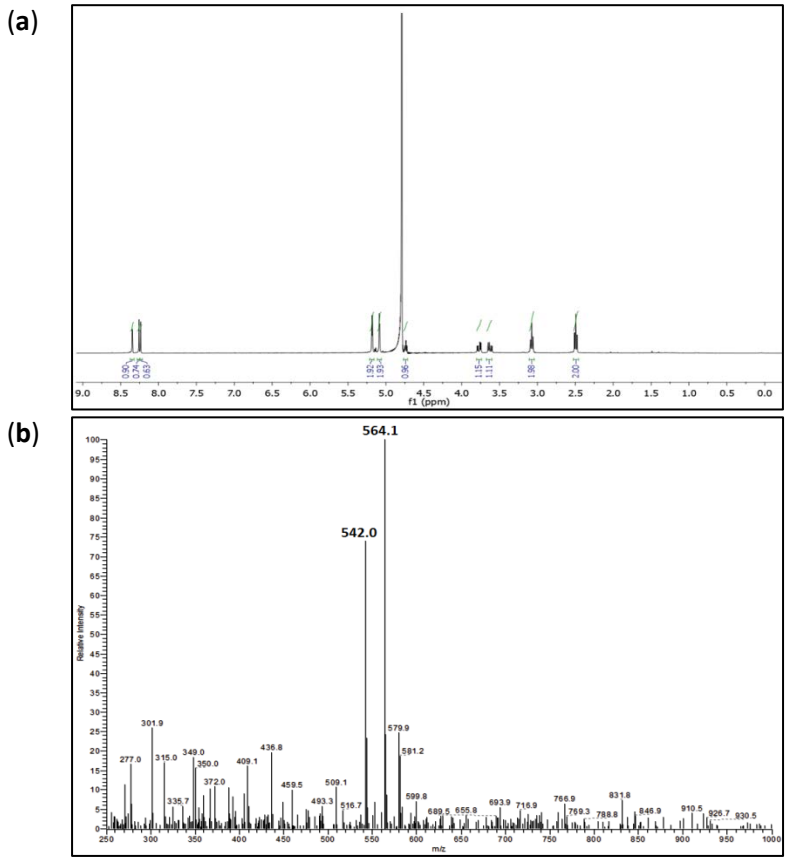

Figure s4. (a) ^{1}H NMR spectrum of $\mathbf{E^{AA}}$ in D_2O. (b) ESI-MS of $\mathbf{E^{AA}}$. Calculated m/z = 542 $[M+H]^+$, 564 $[M+Na]^+$.

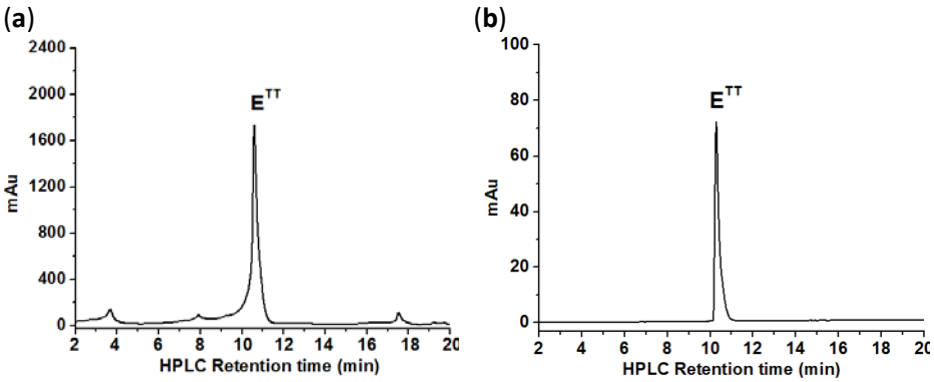

Figure s5. HPLC chromatograms of $\mathbf{E^{TT}}$. (a) Crude; (b) After purification.

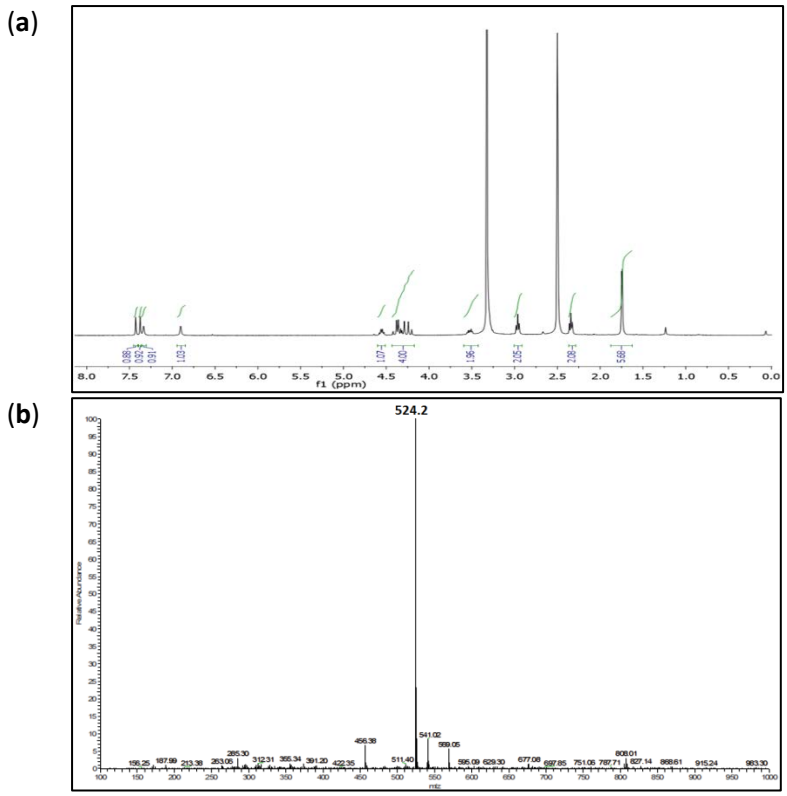

Figure s6. (a) ^{1}H NMR spectrum of $\mathbf{E^{TT}}$ in DMSO-d6. (b) ESI-MS of $\mathbf{E^{TT}}$. Calculated m/z = 524 $[M+H]^{+}$.

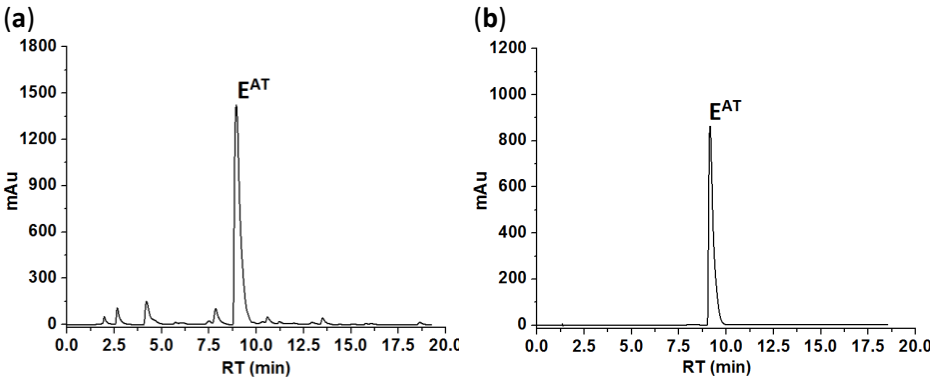

Figure s7. HPLC chromatograms of $\mathbf{E^{AT}}$. (a) Crude; (b) After purification.

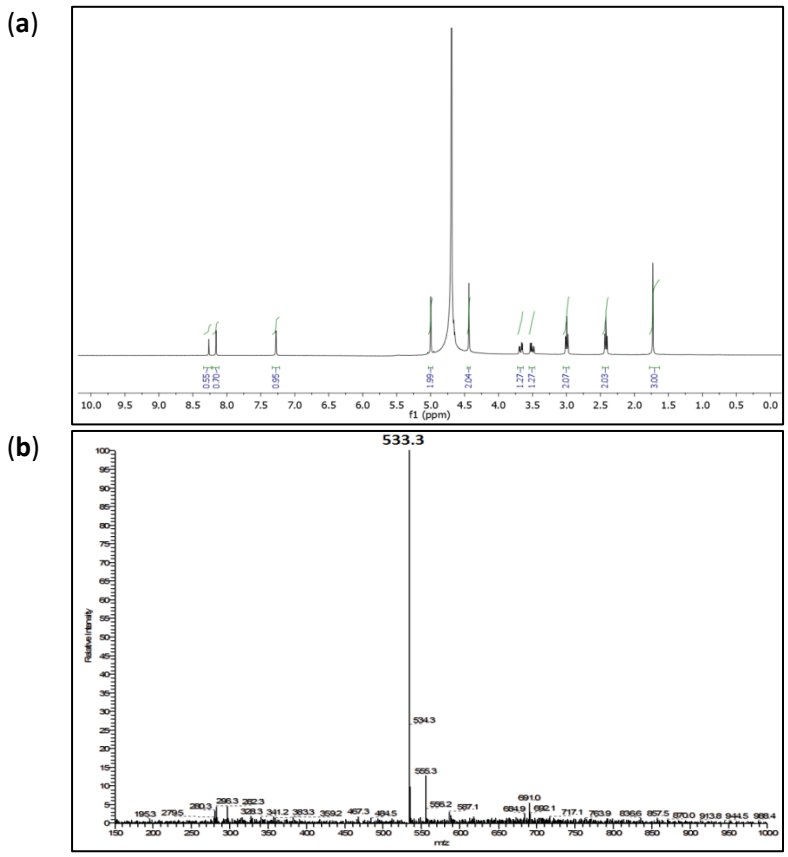

Figure s8. (a) ^{1}H NMR spectrum of $\mathbf{E^{AT}}$ in D_2O. (b) ESI-MS of $\mathbf{E^{AT}}$. Calculated m/z = 533 $[M+H]^+$.

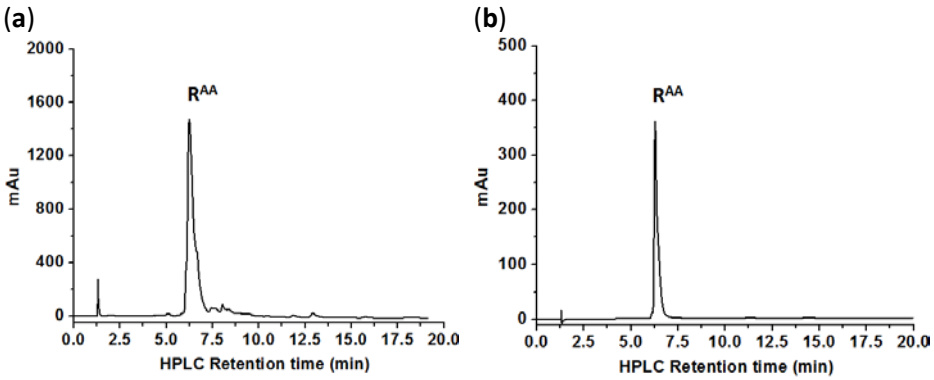

Figure s9. HPLC chromatograms of $\mathbf{R^{AA}}$. (a) Crude; (b) After purification.

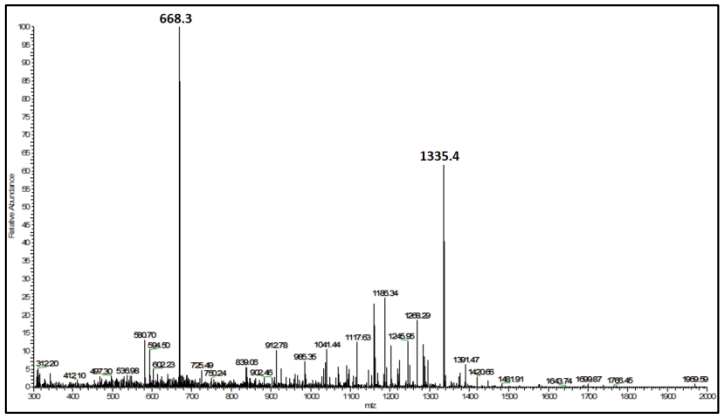

Figure s10. ESI-MS of $\mathbf{R^{AA}}$. Calculated m/z = 1335 $[M+H]^+$.

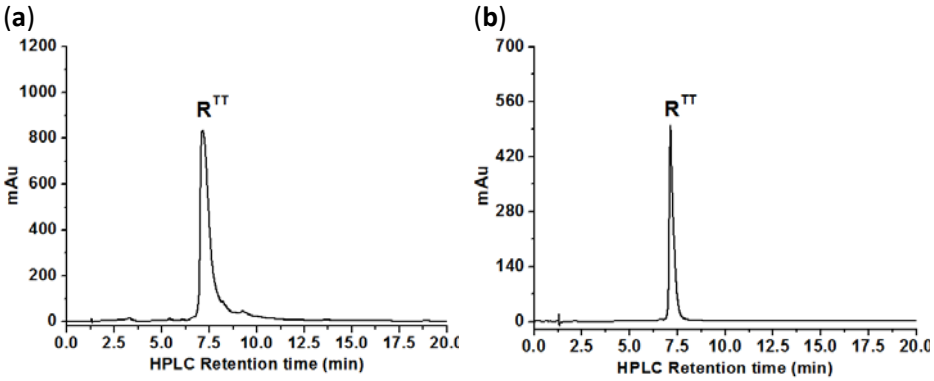

Figure s11. HPLC chromatograms of $\mathbf{R^{TT}}$. (a) Crude; (b) After purification.

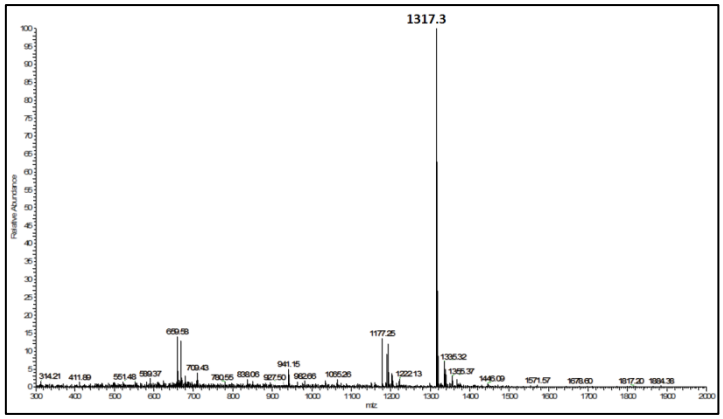

Figure s12. ESI-MS of $\mathbf{R^{TT}}$. Calculated m/z = 1317 $[M+H]^+$.

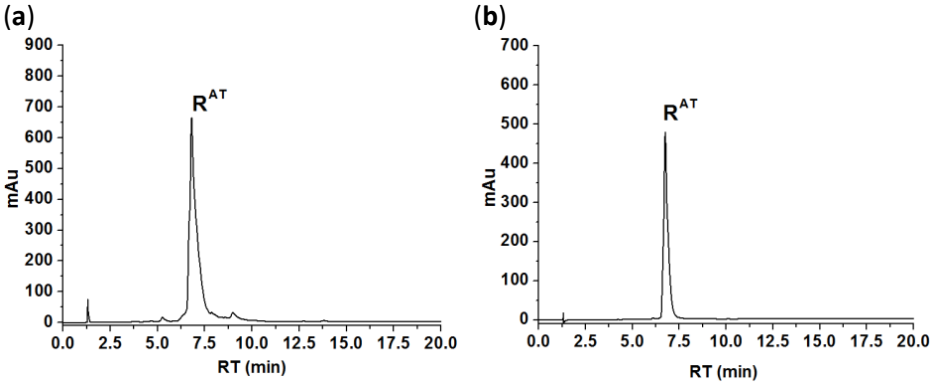

Figure s13. HPLC chromatograms of $\mathbf{R^{AT}}$. (a) Crude; (b) After purification.

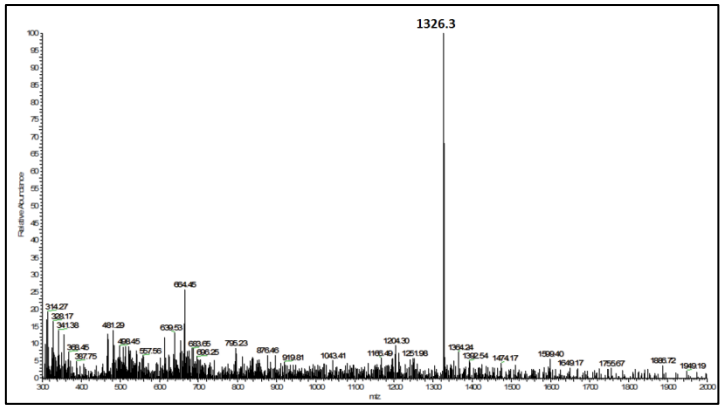

Figure s14. ESI-MS of $\mathbf{R^{AT}}$. Calculated m/z = 1326 $[M+H]^+$.

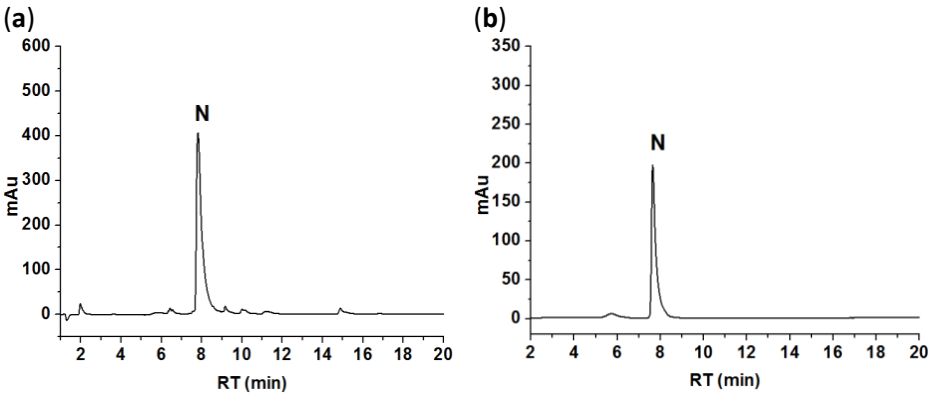

Figure s15. HPLC chromatograms of **N**. (a) Crude; (b) After purification.

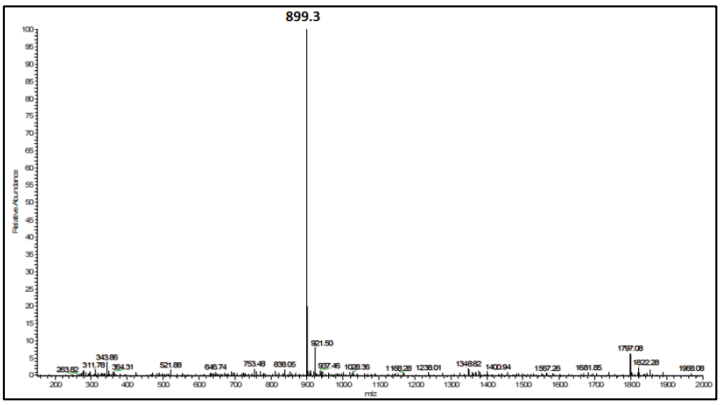

Figure s16. ESI MS of **N**. Calculated m/z = 899 $[M+H]^+$.

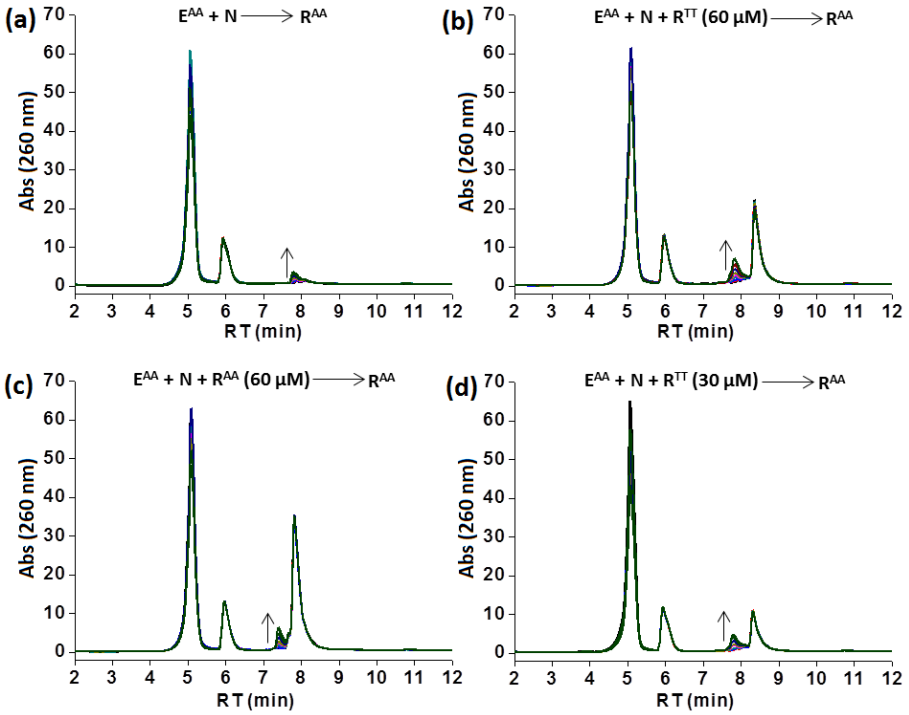

Figure s17. HPLC chromatograms obtained for the replicator-assisted NCL reactions of $\mathbf{E^{AA}}$ with **N**. Experiments were carried out in HEPES buffer pH 7.4 over one hour.

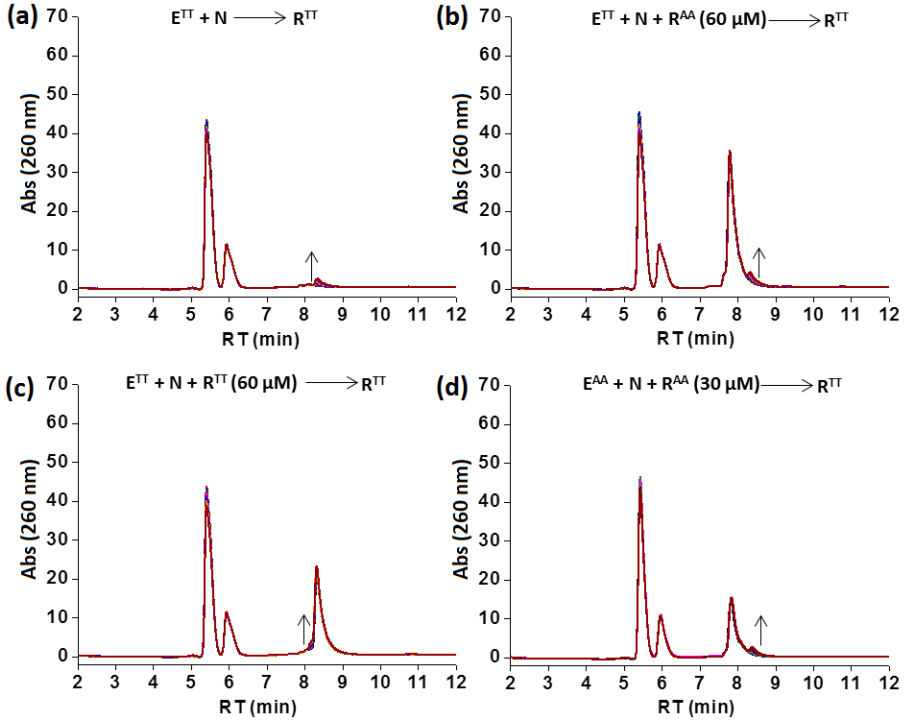

Figure s18. HPLC chromatograms for the replicator-assisted NCL reactions of $\mathbf{E^{TT}}$ with **N**. Experiments were carried out in HEPES buffer pH 7.4 over one hour.

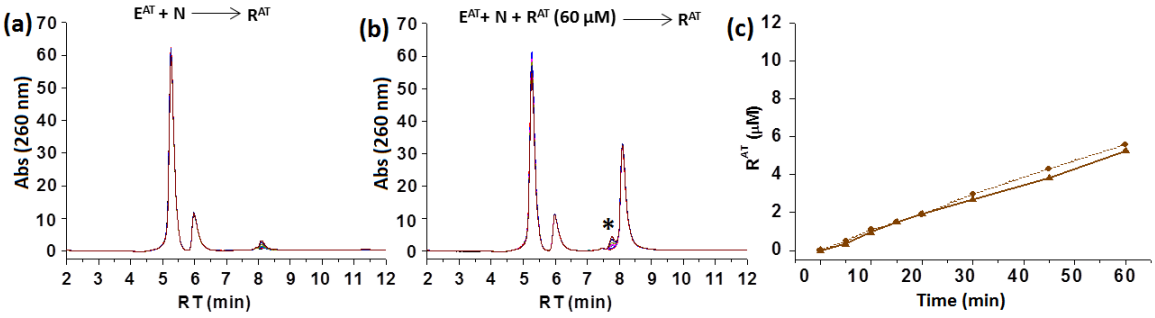

Figure s19. Replication propensity of $\mathbf{R^{AT}}$. a,b) HPLC chromatograms for NCL reactions of $\mathbf{E^{AT}}$ with **N** in background reaction (a) and $\mathbf{R^{AT}}$ seeded reaction (b). (*) in panel (b) marked a minor branched $\mathbf{R^{AT}}$ product. (c) Time dependent formation of $\mathbf{R^{AT}}$ in the background (----) and autocatalytic (—) reactions. Experiments were carried out in HEPES buffer pH 7.4 over one hour.

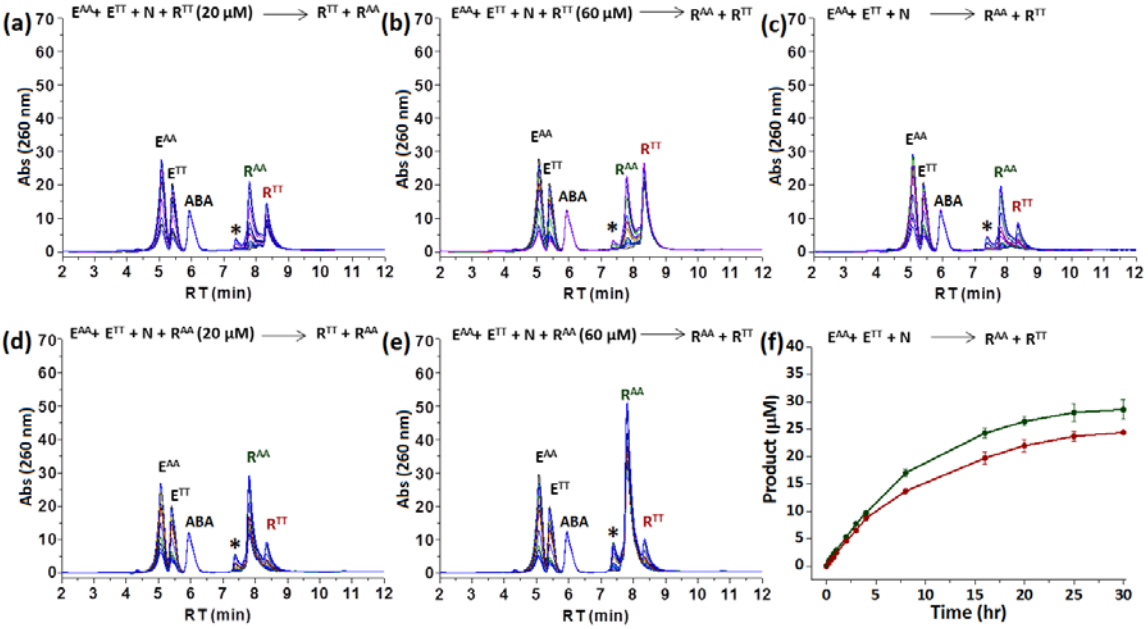

Figure s20. (a-e) HPLC chromatograms for the replicator-assisted NCL of a binary chemical network system in batch reactions. (*) marked a minor branched $\mathbf{R^{AA}}$ product. (f) Time dependent formation of $\mathbf{R^{AA}}$ (*green*) and $\mathbf{R^{TT}}$ (*red*). Experiments were carried out in HEPES buffer pH 7.4 over 30 hours.

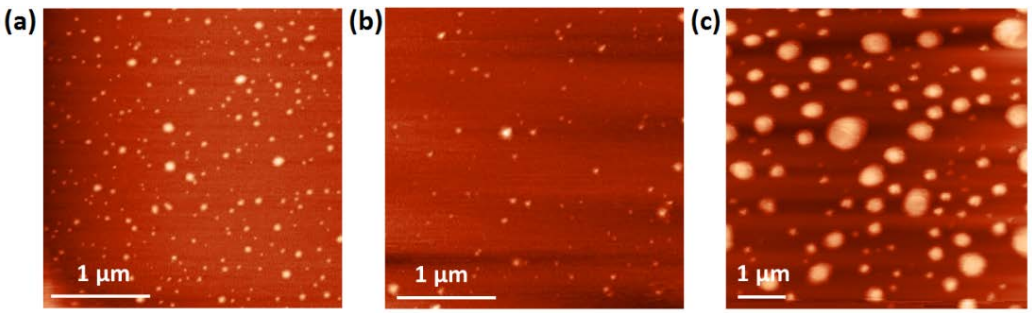

Figure s21. AFM images of the NCL reactants $\mathbf{E^{AA}}$ (a), $\mathbf{E^{TT}}$ (b) and **N** (c).

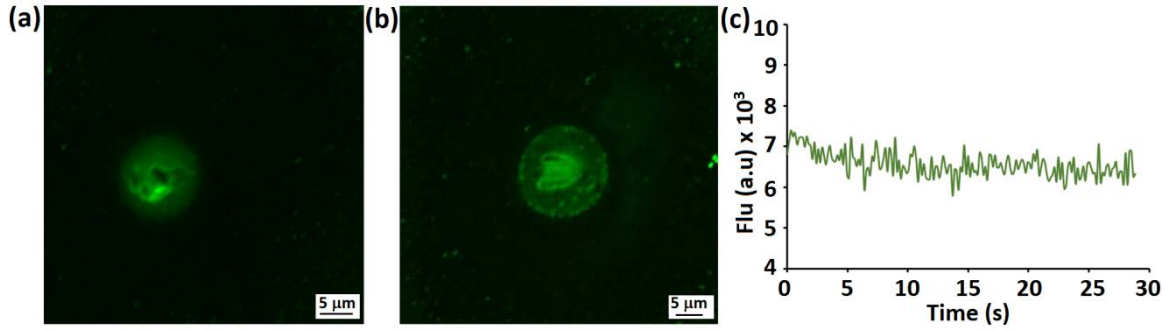

Figure s22. Fluorescence microscopy images of the mixture $\mathbf{R^{AA}}$:$\mathbf{R^{TT}}$ stained with ThT after incubation for 30 min (a) and 2 hr (b). (c) Fluorescence measured for a reference droplet in the FRAP experiment using a 458 nm laser.

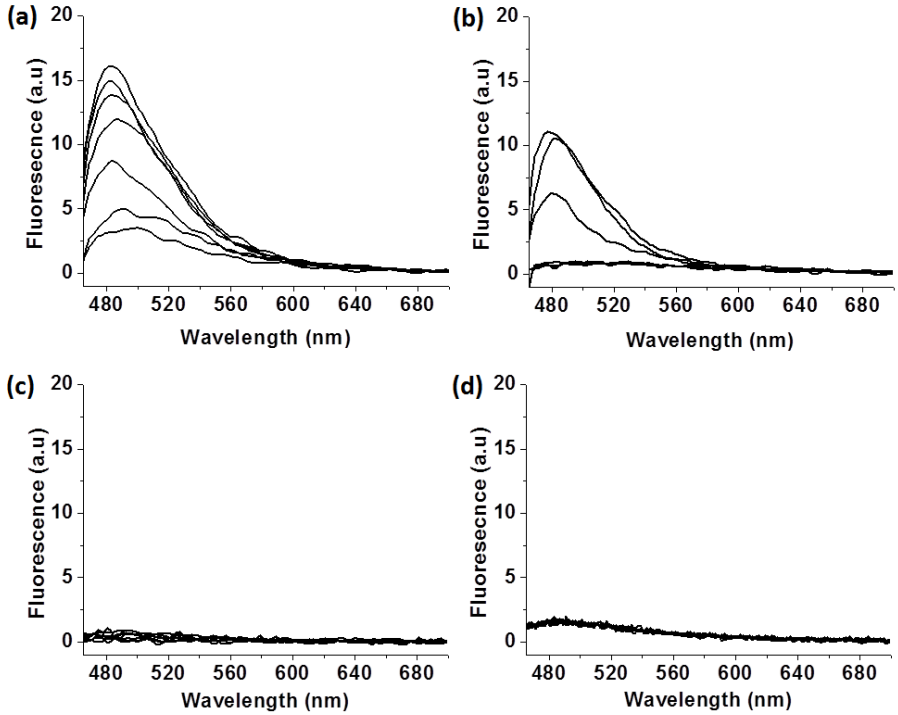

Figure s23. Emission spectra obtained after ThT binding to $\mathbf{R^{AA}}$:$\mathbf{R^{TT}}$ (a), $\mathbf{R^{AA}}$ (b), $\mathbf{R^{TT}}$ (c), and the emission of ThT alone (d). All measurements were carried out in HEPES buffer pH 7.4.

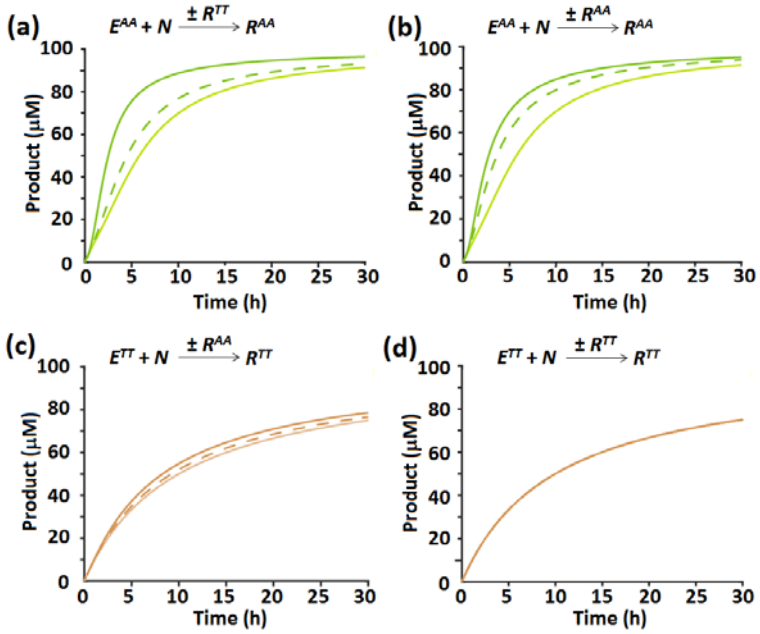

Figure s24. Simulation results of time dependent runs, carried out in line with Figure 1a & 1b of the manuscript. The initial concentrations were: (a) $\boldsymbol{E^{AA}}$ = $\boldsymbol{N}$ = 100 µM and the replicator $\boldsymbol{R^{TT}}$ —(0 µM), – – –(30 µM), —(60 µM); (b) $\boldsymbol{E^{AA}}$ = $\boldsymbol{N}$ = 100 µM and the $\boldsymbol{R^{AA}}$ —(0 µM), – – –(30 µM), —(60 µM); (c) $\boldsymbol{E^{TT}}$ = $\boldsymbol{N}$ = 100 µM and the replicator $\boldsymbol{R^{AA}}$ —(0 µM), – – –(30 µM), —(60 µM); (d) $\boldsymbol{E^{TT}}$ = $\boldsymbol{N}$ = 100 µM and the $\boldsymbol{R^{TT}}$ —(0 µM), – – –(30 µM), —(60 µM).

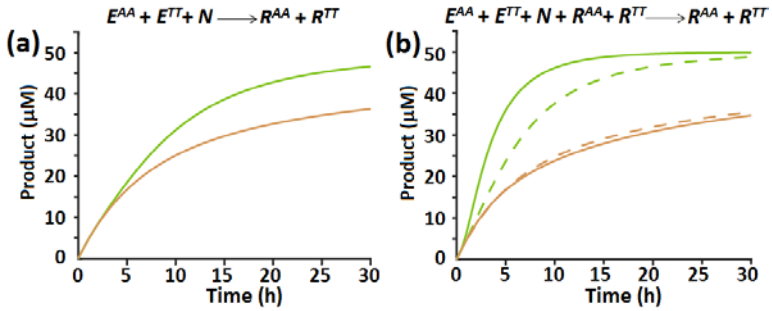

Figure s25. Simulation results of time dependent runs carried out in line with Figure 1c & 1d of the manuscript and the initial concentrations of $\boldsymbol{E^{AA}}$ = $\boldsymbol{E^{TT}}$ = 50 µM, $\boldsymbol{N}$ = 100 µM. (a) Formation of $\boldsymbol{R^{AA}}$ (—) and $\boldsymbol{R^{TT}}$ (—) in the background reaction. (b) Formation of $\boldsymbol{R^{AA}}$ (—), $\boldsymbol{R^{TT}}$ (—) when seeded with $\boldsymbol{R^{AA}}$ = $\boldsymbol{R^{TT}}$ = 30 µM and formation of $\boldsymbol{R^{AA}}$ (— — —), $\boldsymbol{R^{TT}}$ (— — —) when seeded with $\boldsymbol{R^{AA}}$ = $\boldsymbol{R^{TT}}$ = 10 µM each.

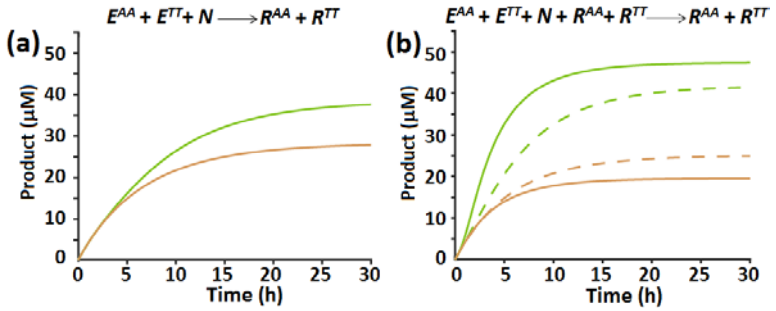

Figure s26. Simulation results of reactions carried out by imposing stringent competition between the two electrophiles E^{AA} and E^{TT} for reacting with N. The initial concentrations were $E^{AA} = E^{TT} = N = 67$ μM. (a) Formation of R^{AA} (—) and R^{TT} (—) in the background reaction. (b) Formation of R^{AA} (—), R^{TT} (—) when seeded with $R^{AA} = R^{TT} = 30$ μM, and formation of R^{AA} (— — —), R^{TT} (— — —) when seeded with $R^{AA} = R^{TT} = 10$ μM each.

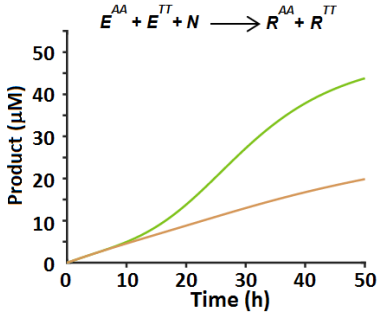

Figure s27. Simulation result of reactions carried out with a slower background reaction (by fixing g = 0.1 instead of g = 1) for longer times. The initial concentrations were $E^{AA} = E^{TT} = 50$ μM, $N = 100$ μM.

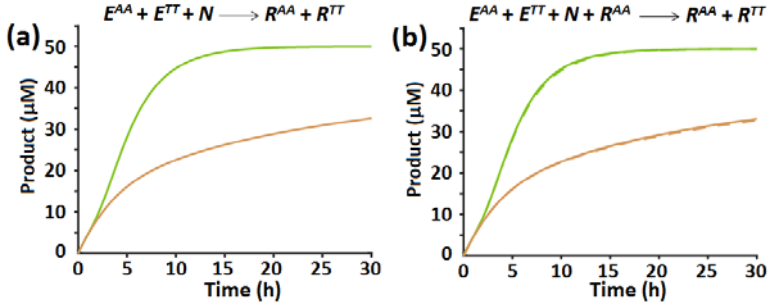

Figure s28. Simulation results of reactions carried out with different minimal seeding ($m_A = 25$, $m_T = 5$) of the replicators and the initial concentrations of $E^{AA} = E^{TT} = 50$ μM, $N = 100$ μM. (a) Formation of R^{AA} (—), R^{TT} (—) in the background reaction. (b) Formation of R^{AA} (—), R^{TT} (—) when seeded with $R^{AA} = 60$ μM and formation of R^{AA} (— — —), R^{TT} (— — —) when seeded with $R^{AA} = 20$ μM.

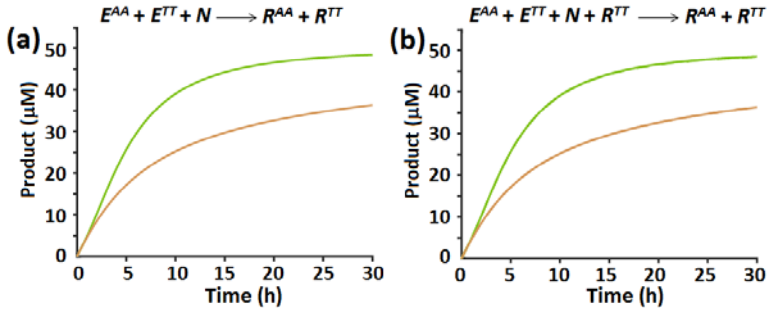

Figure s29. Simulation results of reactions carried out with different minimal seeding (m_A = 5, m_T = 25) of the replicators and the initial concentrations of $\boldsymbol{E^{AA}}$ = $\boldsymbol{E^{TT}}$ = 50 μM, $\boldsymbol{N}$ = 100 μM. (a) Formation of $\boldsymbol{R^{AA}}$ (—), $\boldsymbol{R^{TT}}$ (—) in the background reaction. (b) Formation of $\boldsymbol{R^{AA}}$ (—), $\boldsymbol{R^{TT}}$ (—) when seeded with $\boldsymbol{R^{TT}}$ = 60 μM and formation of $\boldsymbol{R^{AA}}$ (— — —), $\boldsymbol{R^{TT}}$ (— — —) when seeded with $\boldsymbol{R^{TT}}$ = 20 μM.

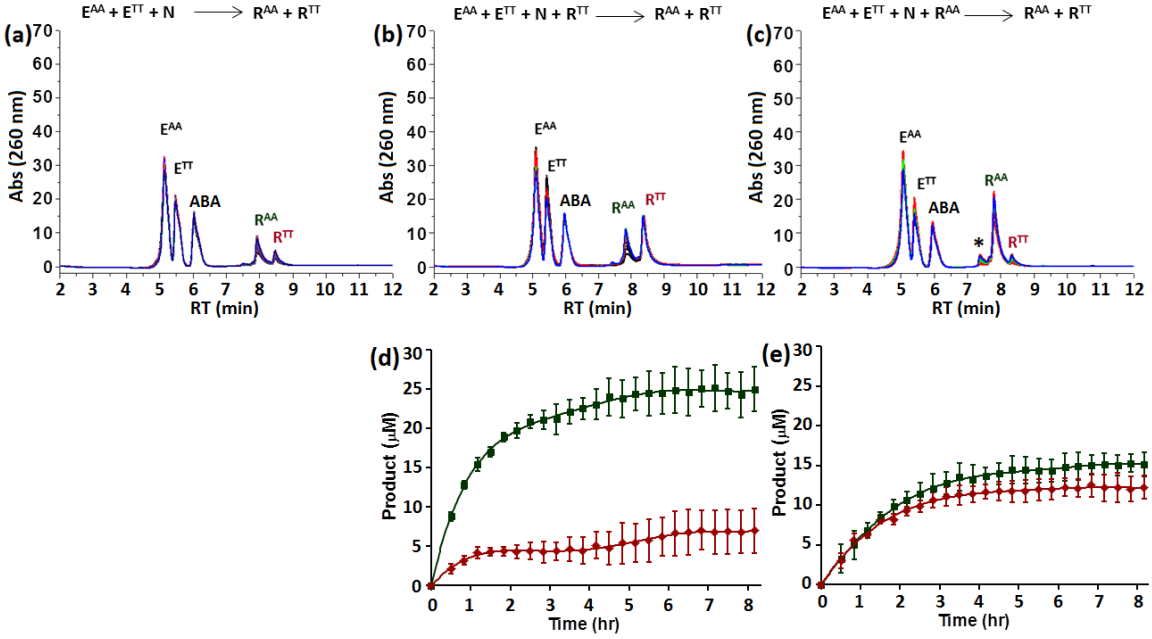

Figure s30. (a-c) HPLC chromatograms for NCL reactions in the binary chemical network (**1:1:2**) carried out in a flow reactor. (a) Background reaction. (b) Seeded with $\mathbf{R^{TT}}$ (20 μM). (c) Seeded with $\mathbf{R^{AA}}$ (20 μM). (*) marked a branched $\mathbf{R^{AA}}$ product. (d) Time dependent formation of $\mathbf{R^{AA}}$ (*green*) and $\mathbf{R^{TT}}$ (*red*) when seeded with $\mathbf{R^{TT}}$ (20 μM). (e) Time dependent formation of $\mathbf{R^{AA}}$ (*green*) and $\mathbf{R^{TT}}$ (*red*) when seeded with $\mathbf{R^{AA}}$ (20 μM). The kinetic profile of the background reaction is shown in Fig. 4b in the manuscript.

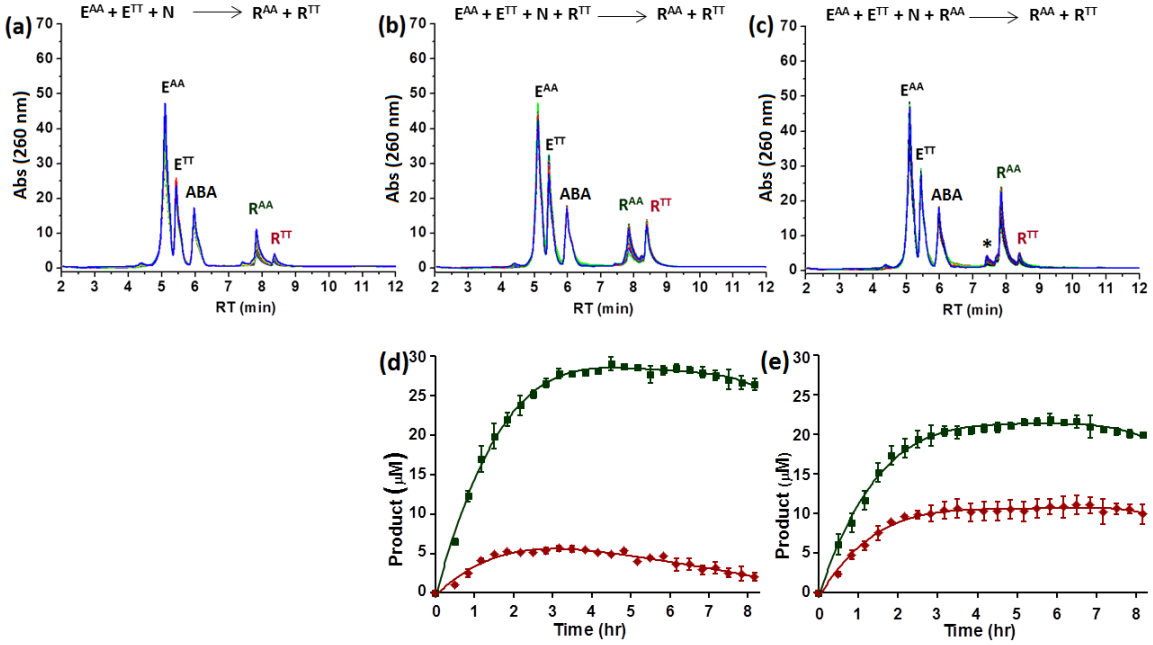

Figure s31. (a-c) HPLC chromatograms for NCL reaction in the binary chemical network (**1:1:1**) carried out in a flow reactor. (a) Background reaction. (b) Seeded with $\mathbf{R^{TT}}$ (20 μM). (c) Seeded with $\mathbf{R^{AA}}$ (20 μM). (*) marked a branched $\mathbf{R^{AA}}$ product. (d) Time dependent formation of $\mathbf{R^{AA}}$ (*green*) and $\mathbf{R^{TT}}$ (*red*) when seeded with $\mathbf{R^{TT}}$ (20 μM). (e) Time dependent formation of $\mathbf{R^{AA}}$ (*green*) and $\mathbf{R^{TT}}$ (*red*) when seeded with $\mathbf{R^{AA}}$ (20 μM). The kinetic profile of the background reaction is shown in Fig. 4c in the manuscript.

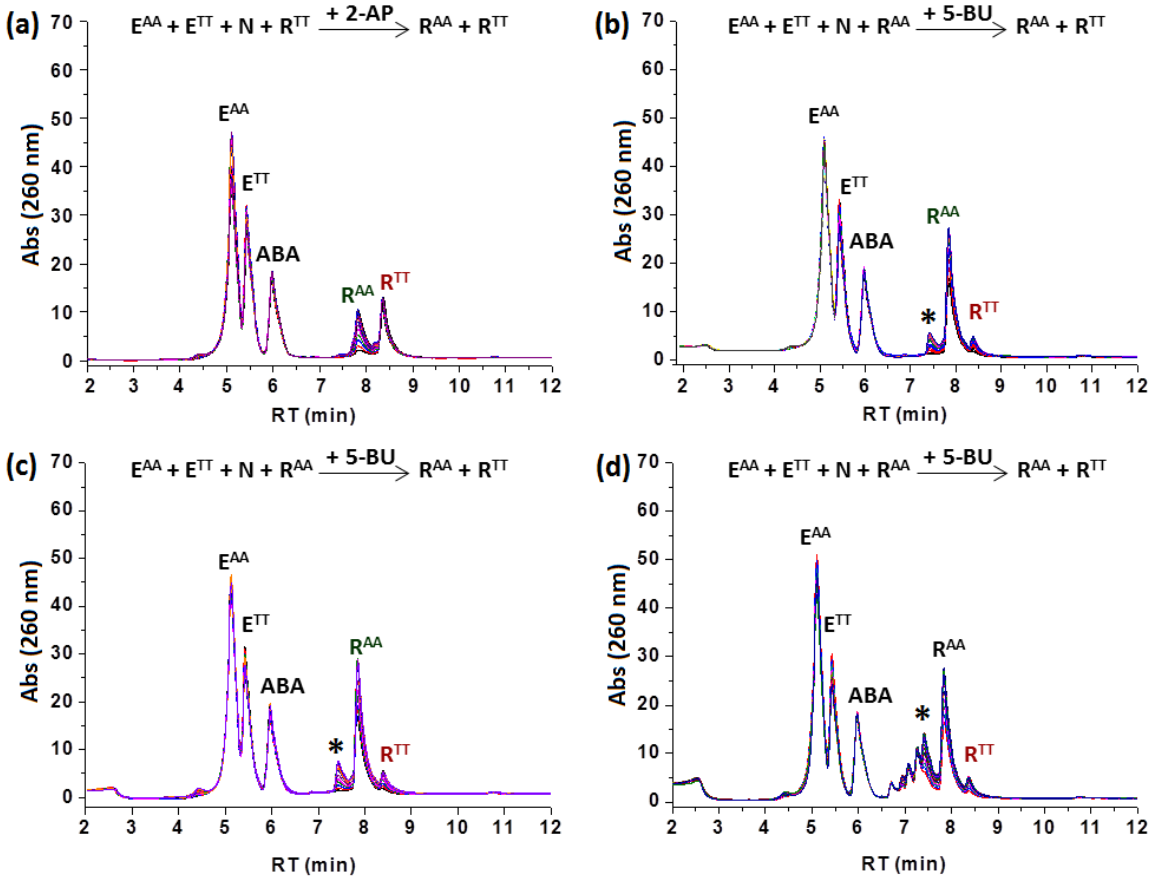

Figure s32. HPLC chromatograms for the replicator-assisted NCL reactions in the binary chemical network (**1:1:1**) carried out in a flow reactor in presence of different inhibitors. (a) 2-AP (40 μM), (b) 5-BU (40 μM), (c) 5-BU (70 μM) and (d) 5-BU (100 μM). (*) marked a branched $\mathbf{R^{AA}}$ product.

Supplementary References

[1] A. Porcheddu, G. Giacomelli, I. Piredda, M. Carta, G. Nieddu, *Eur. J. Org. Chem.* **2008**, 34, 5786–5797.

[2] N. Wagner, G. Ashkenasy, *Chem. Eur. J.* **2009**, 15, 1765–1775.

[3] B. Rubinov, N. Wagner, M. Matmor, O. Regev, N. Ashkenasy, G. Ashkenasy, *ACS nano* **2012**, 6, 7893–7901.

[4] N. Wagner, S. Alasibi, E. Peacock-Lopez, G. Ashkenasy, *J. Phys. Chem. Lett.* **2015**, 6, 60–65.

[5] J. Nanda, B. Rubinov, D. Ivnitski, R. Mukherjee, E. Shtelman, Y. Motro, Y. Miller, N. Wagner, R. Cohen-Luria, G. Ashkenasy, *Nat. Commun.* **2017**, 8, 434.